Int. J. Heat Mass Transfer. Vol. 12, pp. 1141–1155. Pergamon Press 1969. Printed in Great Britain

HEAT AND MASS TRANSFER IN DISPERSED, TWO-PHASE, SINGLE-COMPONENT FLOW

A. U. SIMPSON

AiResearch Manufacturing Division of The Garrett Corporation, Los Angeles, California

K. D. TIMMERHAUS and F. KREITH

University of Colorado, Boulder, Colorado

M. C. JONES

Cryogenics Division—NBS Institute for Materials Research Boulder, Colorado

(*Received* 19 *August and in revised form* 2 *January* 1969)

Abstract—The process of heat transfer to a two-phase mixture of well-dispersed subliming particles and vapor, flowing over a heated surface, is analyzed. It is shown by a laminar boundary layer analysis that, when the surface-area per unit volume of the particle (or solid) phase is large enough, the phase change dominates the heat-transfer process and hastens the development of the thermal boundary layer. Under these conditions, the thermal boundary-layer thickness not only becomes uniform a short distance downstream from the starting point, but also is substantially less than it would be were the particle phase absent. For such systems, the equations describing the heat-transfer process can be considerably simplified and, if the physical properties of both phases are uniform, a remarkably simple solution results. For systems in which the physical properties are not uniform, a solution involving integration across the boundary layer is developed. The solutions are applicable to developing, as well as fully developed, laminar boundary layers over a flat plate; the solutions also approximate conditions in flow through a tube, provided that the tube radius is large compared to the thermal boundary-layer thickness. The predictions of this theoretical analysis agree satisfactorily with experimental results. With slight modification, the same approach may possibly be applicable for turbulent flow in the boundary layer.

NOMENCLATURE

A_p, surface area of particle [cm^2];
A_2, lumped parameter defined by equation (38) [cm$^{\frac{1}{2}}$];
c_{pv}, specific heat of vapor at constant pressure [J/g°K];
D_p, average particle diameter [cm];
E_p, specific internal energy of particle [J/g];
$\mathbf{F}$, vector drag force on average particle [dyn];
g, acceleration due to gravity [cm/s^2];
G, rate of sublimation per unit-volume [g/cm^3 s];
h, height above an arbitrary datum [cm];
h_p, particle heat-transfer coefficient [W/cm^2°K];
h_w, wall heat-transfer coefficient (q_w/Γ), [W/cm^2°K];
H_p, specific enthalpy of solid [J/g];
H_v, specific enthalpy of vapor [J/g];
H_{vs}, specific enthalpy of vapor at saturation temperature [J/g];
k_v, thermal conductivity of vapor at vapor temperature [W/cm°K];
k_{vp}, thermal conductivity of vapor for particle heat transfer [W/cm°K];
k_{vw}, thermal conductivity of vapor for wall heat transfer [W/cm°K];
l, distance from the plate to the outside of the mechanical boundary layer [cm];
m, average particle mass [g];
N, average number of particles per unit volume [1/cm^3];
N_{Nup}, particle Nusselt number (h_pD_p/k_{vp});
p, pressure [dyn/cm^2];
$\dot{Q}_p$, rate of heat transfer to a particle [W/s];

q_w, heat-transfer rate per unit area at wall [W/cm^2];
s, shape factor for particle surface area;
t, real time [s];
T_p, average temperature of the particle [°K];
T_s, saturation temperature [°K];
T_v, vapor temperature [°K];
T_w, tube-wall temperature [°K];
u, velocity parallel to wall [cm/s];
U, free-stream velocity [cm/s];
v, velocity perpendicular to wall [cm/s];
$\mathbf{v}_p$, vector velocity of solid [cm/s];
$\mathbf{v}_v$, vector velocity of vapor [cm/s];
x, distance parallel to wall [cm];
y, distance perpendicular to wall [cm].

Greek symbols

β, drag coefficient for average particle [g/s];
Γ, wall-minus-saturation temperature difference $(T_w - T_s)$ [°K];
δ_m, fluid mechanical boundary-layer thickness [cm];
δ_t, thermal boundary-layer thickness [cm];
ζ, δ_t/δ_m;
η, y/δ_t;
ξ, y/δ_m;
θ, vapor-minus saturation temperature difference $(T_v - T_s)$ [°K];
λ, heat of vaporization or sublimation [J/g];
μ, vapor viscosity at vapor temperature [g/cm s];
μ_{vw}, vapor viscosity related to wall temperature [g/cm s];
ρ_t, density of mixture [g/cm^3];
ρ_p, average mass of particles per unit-volume of mixture [g/cm^3];
$\tilde{\rho}_p$, specific density of particles [g/cm^3];
ρ_v, average mass of vapor per unit-volume of mixture [g/cm^3];
$\tilde{\rho}_v$, specific density of vapor [g/cm^3];
$\boldsymbol{\tau}^*$, stress tensor excluding pressure term [dyn/cm^2];
τ_w, shear stress at wall [dyn/cm^2];
ϕ, rate of change of phase coefficient [g/cm^3 s°K];
ϕ_w, rate of change of phase coefficient at wall [g/cm^3 s°K];
Ψ, conduction heat-transfer rate [W/cm^2];

INTRODUCTION

HEAT transfer by forced convection to a mixture of evaporating drops and vapor at pressures above the triplet point, or to a mixture of subliming particles and vapor at pressures below the triple point, occurs in many systems, such as in mist flow, in drying processes, and in venting cryogenic liquids to outer space. The original purpose of this investigation was to learn more about the heat-transfer characteristics of cryogenic propellants vented to outer space [1] and to explain quantitatively the experimental results of Jones *et al.* [2]. Although illustrative comments below will be directed to a cryogenic mixture of subliming particles and vapor, the analytical approach used is quite general, and its results should be applicable to other engineering systems involving heat transfer by forced convection to dispersed two-phase mixtures.

Forced convection heat transfer to a gas-particle mixture has been studied by Farbar and Depew [3], Tien and Quan [4], Edelman [5] and others. In general, their work shows that the presence of the solid phase enhances the wall heat-transfer coefficient when the particle diameters are less than about 0·01 cm. Change of phase, however, has not been considered in any previous study.

FORMULATION OF THE PROBLEM

To formulate the problem mathematically, the conservation equations for both phases must be considered. If, however, all factors influencing the process were incorporated in the analysis, the problem would become mathematically intractable. On the other hand, in an uncommon system such as the one treated here, it is not

prudent to discard *a priori* a term representing the effect of one of the contributing mechanisms, unless an order-of-magnitude analysis shows that its influence is insignificant. Reference [6] presents the details of the calculations underlying the decision whether or not to include terms in the mathematical formulation of the problem. For cryogenic mixtures, the calculations result in the simplifications listed in Table 1. (For brevity, these calculations are excluded from this paper. For other systems, however, it may be desirable to review the order of magnitude of certain terms.) To avoid unnecessary complications, initial simplifications 1 through 9, whose justification appeared *a posteriori* almost trivial for cryogenic mixtures, are introduced at this stage.

A thermodynamic function is, in general, discontinuous across a phase boundary. Since presently available mathematical techniques can handle only continuous functions, it was necessary to formulate the problem in terms of "bulk" properties, i.e. average properties that take into account the presence of both phases. In conventional terms, this means that the conservation equations are derived by postulating a control-volume for the mixture containing such a large number of particles that (1)

Table 1. *List of simplifications*

Initial simplifications
1. Two phases are initially in thermal equilibrium.
2. Radiation heat-transfer is negligible.
3. Statistical fluctuations in the particle phase density may be averaged.
4. Rotational kinetic energy of the particle phase is negligible.
5. Rotational momentum of the particle phase is negligible.
6. Lift forces on the particles are negligible.
7. Electrostatic forces are negligible.
8. Specific density of the particle phase is constant.
9. Specific density of the particle phase is much greater than specific density of the vapor phase.

Boundary layer simplifications
10. The process is steady-state.
11. Viscous heating is negligible.
12. Relative motion between phases is negligible, except as it affects particle Nusselt number and particle diffusion.
13. Gravitational effects are negligible.
14. The mixture behaves as a Newtonian fluid, with viscosity equal to that of the vapor.
15. The surface of the particle is at local saturation temperature.
16. Temperature gradients in the particle are negligible.
17. Specific heats of the particle and vapor are constant.
18. Flow is two dimensional.
19. Boundary-layer approximations are valid.
20. Pressure gradients are negligible.
21. Vapor viscosity and thermal-conductivity are constant.

Integral solution simplifications
22. Average particle size is uniform.
23. Average particle number-density is uniform.
24. Free-stream velocity gradients are negligible.
25. Changes in bulk densities are negligible.
26. Effects of free-stream turbulence are negligible.
27. Particle-wall interactions are negligible.
28. Polynomial approximations of velocity and temperature profiles in boundary layer are valid (necessary for solution).
29. Two phases are in thermal equilibrium outside the thermal boundary-layer.
30. Thermal and fluid-mechanical boundary-layers start at the same point.
31. Particle Nusselt number is constant.
32. Particle Nusselt number is not affected by mass transfer.

particle properties may be treated as continuous functions and (2) statistical fluctuations can be averaged. At the same time, the volume can conceptually be made arbitrarily small so that mathematical derivatives exist. This approach is actually only an extension of the assumption usually made in continuum mechanics in which all physical properties are treated as continuous functions while, in reality, any physical material consists of particles having discrete energy levels. A schematic diagram illustrating the specific process treated in this study, as well as some of the symbols used in the analysis below, are shown in Fig. 1.

$\rho_p = Nm$. If it is assumed that the equivalent average number of particles, as well as the average net mass, is conserved, the conservation-of-mass equations for particle and vapor can be written in the form

(Solid)

$$\frac{\partial \rho_p}{\partial t} + \nabla \cdot \rho_p \mathbf{v}_p - N\frac{Dm}{Dt} = 0 \tag{1}$$

and

(Vapor)

$$\frac{\partial \rho_v}{\partial t} + \nabla \cdot \rho_v \mathbf{v}_v + N\frac{Dm}{Dt} = 0. \tag{2}$$

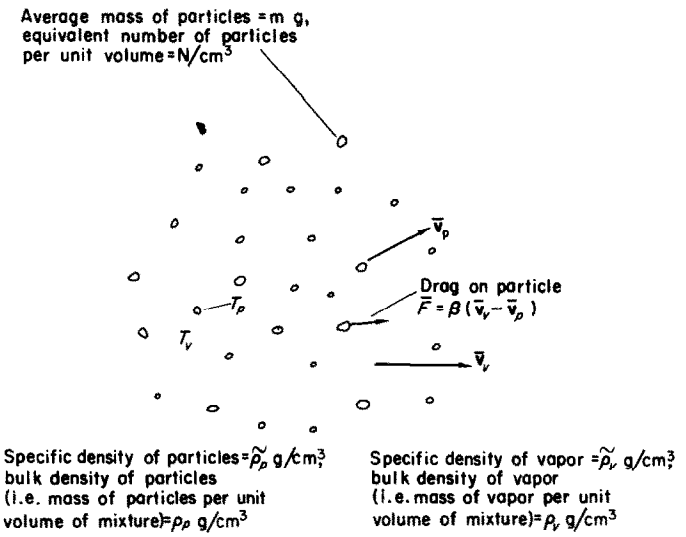

FIG. 1. Schematic of particle-vapor flow, with definition of some symbols.

Conservation of mass

Let $N(\bar{r}, t)$ be the equivalent average number of particles per unit volume. The qualification "equivalent" is used to indicate that particle identities are not lost. For example, if two particles collide and stick together, then the number of particles is still counted as two. Similarly, if a particle completely sublimes, it is still counted as a particle, but its mass is zero. The function N is related to the average bulk density of the solid phase $\rho_p(\bar{r}, t)$, and the average mass of a particle m according to

Conservation of momentum

The forces between the two phases result from their relative motion. To evaluate these forces, it is convenient to define an average particle-drag coefficient β according to the equation

$$\frac{D}{Dt}(m\mathbf{v}_p) = \beta(\mathbf{v}_v - \mathbf{v}_p) - mg\nabla h. \tag{3}$$

Expanding the substantial derivative in the foregoing equation and using the definition of ρ_p given above yields the conservation-of-momentum equation for the solid phase

(Solid)

$$\rho_p \frac{D\mathbf{v}_p}{Dt} + \mathbf{v}_p N \frac{Dm}{Dt} - \beta N(\mathbf{v}_v - \mathbf{v}_p) + \rho_p g \nabla h = 0. \tag{4}$$

It is possible, as shown in detail in [6], to derive a similar conservation-of-momentum equation for the mixture. When the conservation-of-momentum equation for the solid or particle phase is subtracted from it, the conservation of momentum for the vapor phase is found to be

(Vapor)

$$\rho_v \frac{D\mathbf{v}_v}{Dt} - \mathbf{v}_v N \frac{Dm}{Dt} + \beta N(\mathbf{v}_v - \mathbf{v}_p) + \nabla p - \nabla \cdot \tau^* + g\rho_v \nabla h = 0. \tag{5}$$

Conservation of energy

If we define an average particle heat transfer coefficient h_p and an average specific particle density $\tilde{\rho}_p$ for the solid phase and assume that each particle is sufficiently regular so that its surface area is proportional to its volume to the two-thirds power, as in a sphere, the surface area of a particle is

$$A_p = (36\pi)^{\frac{1}{3}} s \left(\frac{m}{\tilde{\rho}_p}\right)^{\frac{2}{3}}, \tag{6}$$

where s is a particle-shape factor equal to unity for a sphere. The rate of heat transfer between a particle and the surrounding vapor is given by

$$\dot{Q}_p = (36\pi)^{\frac{1}{3}} s \left(\frac{m}{\tilde{\rho}_p}\right)^{\frac{2}{3}} h_p(T_v - T_p). \tag{7}$$

Since heat transfer to a particle causes sublimation, as well as a change in the internal energy of the solid, conservation of energy demands that

$$\lambda \frac{Dm}{Dt} - m \frac{DE_p}{Dt} + (36\pi)^{\frac{1}{3}} s \left(\frac{m}{\tilde{\rho}_p}\right)^{\frac{2}{3}} h_p(T_v - T_p) = 0. \tag{8}$$

The internal energy term can be replaced by the enthalpy of the solid, because the solid density is uniform; thus, extending equation (8) to N particles per unit volume yields the conservation-of-energy equation for the solid phase

(Solid)

$$\lambda N \frac{Dm}{Dt} - \rho_p \frac{DH_p}{Dt} + \frac{6s}{D_p} \frac{\rho_p}{\tilde{\rho}_p} h_p(T_v - T_p) = 0. \tag{9}$$

where the term $6s/D_p$ corresponds to the ratio of particle area to volume. The conservation equation for the vapor is derived by obtaining a conservation equation for the mixture and subtracting from it equation (9). After some rearrangement, this yields

(Vapor)

$$N \frac{Dm}{Dt} \{\tfrac{1}{2}(\mathbf{v}_4 \cdot \mathbf{v}_v - \mathbf{v}_p \cdot \mathbf{v}_p) - (H_v - H_{vs})\} + \frac{6s}{D_p} \frac{\rho_p}{\tilde{\rho}_p} h_p(T_v - T_p) + \rho_v \frac{DH_v}{Dt} - \frac{Dp}{Dt} - N\beta(\mathbf{v}_v - \mathbf{v}_p) \cdot (\mathbf{v}_v - \mathbf{v}_p) - \tau^* \cdot \nabla \mathbf{v}_v - \nabla(k_v \nabla T_v) = 0. \tag{10}$$

It should be noted that the conservation equations are coupled with the change-of-phase term $N(dm/dt)$. Moreover, although no relative-motion terms appear in the equations because their order of magnitude is negligible, the value of h_p (the particle heat-transfer coefficient) still depends on the relative motion between the two phases.

BOUNDARY-LAYER APPROXIMATIONS

Numerical solutions of equations (1), (2), (4), (5), (9), and (10) would be complicated and require prohibitive computer time. Instead, analytical solutions will be formulated by means of the boundary-layer integral method [8–10]. To use this method simplifications 10 through 21 in Table 1 are introduced, and equations (1), (2), (4), (5), (9), and (10) simplify respectively to the following boundary-layer forms:

Conservation of mass

(Solid)

$$\frac{\partial}{\partial x}(\rho_p u) + \frac{\partial}{\partial y}(\rho_p v) - G = 0 \qquad (11)$$

and

(Vapor)

$$\frac{\partial}{\partial x}(\rho_v u) + \frac{\partial}{\partial y}(\rho_v v) + G = 0. \qquad (12)$$

Conservation of momentum

(Solid)

$$\rho_p u \frac{\partial u}{\partial x} + \rho_p v \frac{\partial u}{\partial y} + uG = 0 \qquad (13)$$

and

(Vapor)

$$\rho_v u \frac{\partial u}{\partial x} + \rho_v v \frac{\partial u}{\partial y} - uG - \mu \frac{\partial^2 u}{\partial y^2} = 0. \qquad (14)$$

Conservation of energy

(Solid)

$$\frac{6s}{D_p}\frac{\rho_p}{\tilde{\rho}_p} h_p(T_v - T_s) + \lambda G = 0 \qquad (15)$$

and

(Vapor)

$$\rho_v c_{pv} u \frac{\partial T_v}{\partial x} + \rho_v c_{pv} v \frac{\partial T_v}{\partial y} + \frac{6s}{D_p}\frac{\tilde{\rho}_p}{\tilde{\rho}_p} h_p(T_v - T_s) - c_{pv}(T_v - T_s) G - k_v \frac{\partial^2 T_v}{\partial y^2} = 0. \qquad (16)$$

The coupling term between equations (11) through (16) is G, the rate of sublimation per unit volume. This term is given explicitly by Equation (15).

To proceed with the integral method and integrate across the boundary layers, simplifications 22 through 32 are introduced. The process can then be visualized as shown schematically in Fig. 2. In this figure the vertical scale has been greatly expanded. For the cryogenic mixture under consideration here, order-of-magnitude dimensions are 50 cm for the horizontal length, 0·1 cm for the thermal boundary-layer thickness, 0·25 cm for the mechanical boundary-layer thickness, 0·003 cm for the particle diameter, and 0·03 cm for the distance between particle centers. Thus, the thermal boundary-layer thickness is about three times greater than the distance between particles.

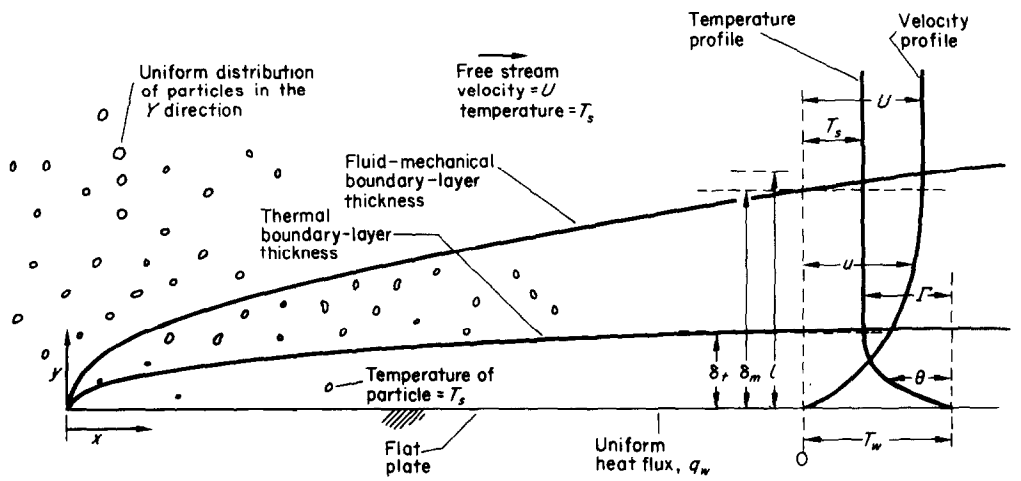

FIG. 2. Boundary-layer model.

Integral equations

With Leibnitz's rule for differentiation of integrals, equation (12) can be partially integrated with respect to y to give

$$\frac{\partial}{\partial x}\int_0^l \rho_v u\,dy + \rho_v v(l) + \int_0^l G\,dy = 0. \quad (17)$$

Also, with the addition of the two conservation-of-mass equations [equations (11) and (12)] and with partial integration, one can verify that

$$\frac{\partial}{\partial x}\int_0^l \rho_t u\,dy + \rho_t v(l) = 0, \quad (18)$$

where l is the perpendicular distance from the flat plate to some point outside both the fluid-mechanical and thermal-boundary layers.

Two additional equations may be obtained from the sum of equations (11) and (12) and also from equation (12) by multiplying these equations by u and $c_{pv}T_v$, respectively, and integrating. This procedure results in

$$\int_0^l \rho_t u\frac{\partial u}{\partial x}dy + \int_0^l \rho_t u\,dv = 0 \quad (19)$$

and

$$\int_0^l \rho_v c_{pv}T_v\frac{\partial u}{\partial x}dy + \int_0^l \rho_v c_{pv}T_v\,dv + \int_0^l c_{pv}T_v G\,dy = 0. \quad (20)$$

Adding and integrating the conservation-of-momentum equations [equations (13) and (14)] gives

$$\int_0^l \rho_t u\frac{\partial u}{\partial x}dy + \rho_t U v(l) - \int_0^l \rho_t u\,dv = -\mu_{vw}\left.\frac{\partial u}{\partial y}\right|_{y=0}. \quad (21)$$

Substituting from equations (18) and (19) for the second and third terms in equation (21), and changing the limits to 0 to δ_m (since the integrals from δ_m to l are zero) yields the momentum integral equation

$$\tau_w = \mu_{vw}\left.\frac{\partial u}{\partial y}\right|_{y=0} = \frac{\partial}{\partial x}\int_0^{\delta_m} \rho_t U^2\frac{u}{U}\left(1-\frac{u}{U}\right)dy. \quad (22)$$

For conservation of energy, adding and integrating equations (15) and (16) yields

$$\int_0^l \rho_v c_{pv}u\frac{\partial T_v}{\partial x}dy + \rho_v c_{pv}v(l)\,T_s - \int_0^l \rho_v c_{pv}T_v\,dv - \int_0^l \lambda G\,dy - \int_0^l c_{pv}(T_v - T_s)\,G\,dy = q_w. \quad (23)$$

Substituting from equations (17) and (20) for the second and third terms in equation (23), and changing the limits to 0 to δ_t (since the integrals from δ_t to l are zero) yields the energy integral equation

$$q_w = \frac{\partial}{\partial x}\int_0^{\delta_t} \rho_v c_{pv}u\theta\,dy + \int_0^{\delta_t} \phi\lambda\theta\,dy, \quad (24)$$

where

$$\phi = \frac{1}{\lambda}\frac{6s}{D_p}\frac{\rho_p}{\tilde{\rho}_p}h_p = \frac{Ns\pi D_p^2 h_p}{\lambda}. \quad (25)$$

The term ϕ is the coefficient of rate of change-of-phase, i.e. the rate of change-of-phase per unit volume and per unit of temperature difference between the vapor and particles.

POLYNOMIAL APPROXIMATIONS

The choice of polynomials with which to approximate the velocity and temperature profiles is to some extent arbitrary. Fourth-degree polynomials satisfy the boundary conditions

very well, but a relatively complicated solution ensues in which the coefficients of the temperature polynomials are functions of the thermal boundary-layer thickness. However, if third-degree polynomials are used, one obtains remarkably simple solutions.

The boundary conditions to be satisfied are:

$$u(0) = 0, \quad v(0) = 0, \quad u(\delta_m) = U, \quad \left.\frac{\partial u}{\partial y}\right|_{\delta_m} = 0,$$

$$\theta(0) = \Gamma, \quad \theta(\delta_t) = 0, \left.\frac{\partial T_v}{\partial y}\right|_{\delta_t} = 0,$$

$$\text{and} \left.\frac{\partial^2 T_v}{\partial y^2}\right|_{\delta_t} = 0;$$

these conditions yield polynomial approximations for the velocity and temperature distributions,

(Velocity)

$$\frac{u}{U} = \frac{3\xi}{2} - \frac{\xi^3}{2} \tag{26}$$

and

(Temperature)

$$\frac{\theta}{\Gamma} = 1 - 3\eta + 3\eta^2 - \eta^3 \tag{27}$$

where $\xi = y/\delta_m$ and $\eta = y/\delta_t$.

From equation (27) the heat-transfer coefficient is related to the thermal boundary-layer thickness according to the relation

$$h_w = \frac{q_w}{\Gamma} = \frac{3k_{vw}}{\delta_t} \tag{28}$$

which shows that a solution for δ_t also yields a direct solution for h_w. Substituting the polynomial approximation for velocity [equation (26)] in the momentum integral equation [equation (22)] results in

$$\frac{3}{2}\frac{U}{\delta_m}\mu_{vw} = \frac{\partial}{\partial x}\int_0^{\delta_m} \rho_t U^2 \left(\frac{3\xi}{2} - \frac{\xi^3}{2}\right) \times \left(1 - \frac{3\xi}{2} + \frac{\xi^3}{2}\right) dy. \tag{29}$$

Performing the indicated operations and replacing the partial derivative by a total derivative gives

$$\frac{d\delta_m}{dx} = \frac{140}{13}\frac{\mu_{vw}}{\delta_m \rho_t U}. \tag{30}$$

The velocity and temperature polynomial approximations [equations (26) and (27)] can be substituted in the energy integral equation [equation (24)] to yield

$$q_w = \frac{\partial}{\partial x}\int_0^{\delta_t} \rho_v c_{pv}\frac{U}{2}(3\xi - \xi^3)\frac{\delta_t q_w}{3k_{vw}}(1 - 3\eta + 3\eta^2 - \eta^3)\,dy + \int_0^{\delta_t} \phi\lambda\frac{\delta_t q_w}{3k_{vw}}(1 - 3\eta + 3\eta^2 - \eta^3)\,dy. \tag{31}$$

Performing the indicated operations, dividing by q_w, and replacing the partial derivative by a total derivative gives

$$1 = \frac{\rho_v c_{pv} U}{6k_{vw}}\frac{d}{dx}\left\{\delta_t^2\zeta\left(\frac{3}{20} - \frac{1}{140}\zeta^2\right)\right\} + \frac{\phi\lambda\delta_t^2}{12k_{vw}} \tag{32}$$

where

$$\zeta = \frac{\delta_t}{\delta_m}. \tag{33}$$

If the thermal boundary-layer thickness is less than the fluid-mechanical boundary-layer thickness it may be assumed that $\zeta < 1$; then

$$\frac{1}{140}\zeta^2 \ll \frac{3}{20}. \tag{34}$$

Dropping the negligible term in equation (32) and using the chain rule for differentiation finally gives

$$\frac{d\delta_t}{dx} = \frac{\delta_t}{3\delta_m}\frac{d\delta_m}{dx} + \frac{40}{3}\frac{k_{vw}}{\rho_v c_{pv} U}\frac{\delta_m}{\delta_t^2} - \frac{10}{9}\frac{\lambda\phi_w}{\rho_v c_{pv} U}\delta_m. \tag{35}$$

It is evident from equations (30) and (35) that the gradients of the boundary layers are indeterminate at $x = 0$ because $\delta_m(0) = 0$; thus numerical integration cannot be started at $x = 0$. Use of L'Hospital's rule, however, shows that, when $x \to 0$, the fourth term in equation (35) goes to zero, whereas the other three terms go to infinity. Also, if one neglects variations in viscosity near $x = 0$, equation (30) can be integrated to obtain δ_m as

$$\delta_m = \frac{280\,\mu_{vw}x}{(13\ \rho_t U)}^{\frac{1}{2}}, \qquad x \to 0. \tag{36}$$

Substituting δ_m from equation (36) and $d\delta_m/dx$ from equation (30) into equation (35) gives

$$\frac{d\delta_t}{dx} = \frac{1}{6}\frac{\delta_t}{x} + A_2\frac{x^{\frac{1}{2}}}{\delta_t^2}, \qquad x \to 0, \tag{37}$$

where

$$A_2 = 61{\cdot}6\,\frac{k_{vw}}{\rho_v c_{pv} U}\,\frac{u_{vw}}{\rho_t U}^{\frac{1}{2}}. \tag{38}$$

Equation (37) is a form of Bernoulli's equation, and can be reduced to a linear ordinary-differential equation by forming the derivative of $\delta_t^3/x^{\frac{1}{2}}$.

Integration then yields for small values of x

$$\delta_t = x^{\frac{1}{2}}(3A_2)^{\frac{1}{3}}, \qquad x \to 0. \tag{39}$$

Equations (36) and (39) can now be used to obtain values of δ_m and δ_t approaching $x = 0$. These values of δ_m and δ_t serve as starting values for numerical integration of equations (30) and (35).

SOLUTIONS

Numerical solutions of equations (30), (35), (36) and (39) to determine the shape and relative magnitudes of δ_m and δ_t were obtained by Simpson [6] using the Adams–Moulton predictor–corrector method; a typical solution is shown in Fig. 3. The thermal boundary-layer thickness becomes almost constant a few centimeters from the start of the boundary layers. (The slight rate of growth of the thermal boundary layer appears to have been caused in this case by the incorporation in the integration procedure of variations of fluid properties along

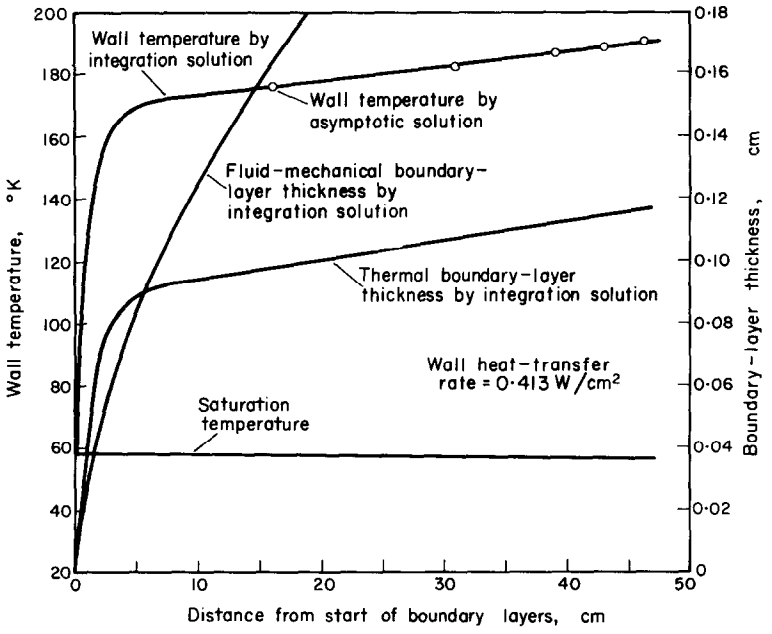

FIG. 3. Typical integration-solution for nitrogen.

the boundary layer.) This suggests that the first term ($d\delta_t/dx$) in equation (35) is negligible for large values of x.

The integration solution also shows that $\delta_t \ll \delta_m$ for large values of x. Consequently, the second term in equation (35) can be expected to be negligible for large values of x.

Equating the third and fourth terms in equation (35) to zero yields the asymptotic solution. It can easily be verified that the terms δ_m, ρ_v, c_{pv} and U cancel and

$$\delta_t \simeq \left(\frac{12k_{vw}}{\phi\lambda}\right)^{\frac{1}{2}}, \qquad x > 10. \tag{40}$$

Substituting the results of equation (40) and the definition of ϕ from equation (25) into equation (28) and using the definition of the particle Nusselt number ($N_{Nup} = h_p D_p/k_{vp}$) gives

$$h_w = \frac{1}{D_p}\left(\frac{9s}{2}\frac{\rho_p}{\tilde{\rho}_p} N_{Nup} k_{vw} k_{vp}\right)^{\frac{1}{2}}, \qquad x > 10. \tag{41}$$

Note that the particle Nusselt number asymptotically approaches 2·0 as the relative motion between the phases goes to zero [8]. The asymptotic limit of the particle Nusselt number of 2·0 for zero relative motion between phases seems reasonable since the Nusselt number for a sphere in pure conduction can be calculated to be 2·0.

Numerical values of the heat-transfer coefficient at the wall calculated using the integration and the asymptotic solutions were compared by Simpson [6] and found to differ by less than one per cent for x greater than 10 cm. This implies, for the cases studied, the validity of the assumptions that the first and second terms in equation (35) are negligible for $x > 10$; it also implies that the thermal boundary layer rapidly becomes fully developed, i.e. in about five tube diameters.

The absence of δ_m and U in the asymptotic solution suggests that convection heat transfer is not an important factor when the thermal boundary layer is fully developed. Thus, the mechanism should correspond closely with that of heat transfer to a stagnant mixture. A stagnant mixture is defined as having zero velocity parallel to the wall, but also, due to generation of vapor, having its interface move perpendicular to the wall. Partial derivatives with respect to time do not appear in the integration and asymptotic solutions, since steady-state conditions exist. Thus, in order that the stagnant-model solution can correspond with the integration and asymptotic solutions, steady-state conditions must be imposed on the stagnant model. This corresponds to a physical situation in which a large proportion of the heat transferred to the stagnant mixture is absorbed by the change in phase, only a small quantity of heat goes to raise the temperature of the vapor and its rate of increase may be neglected. From equations (2) and (10), the stagnant model is described in two dimensions by the following relationships:

$$\frac{dv}{dy} = \frac{1}{\rho_v}\left(\phi\theta - v\frac{d\rho_v}{dT_v}\frac{d\theta}{dy}\right), \tag{42}$$

$$\frac{d\psi}{dy} = -\rho_v c_{pv} v\frac{d\theta}{dy} - \phi\theta(\lambda + c_{pv}\theta), \tag{43}$$

and

$$\frac{d\theta}{dy} = -\frac{\psi}{k_v}. \tag{44}$$

Because equations (42), (43) and (44) are less complicated than those leading to the integration and asymptotic solutions, it is feasible to include in the analysis the variation of physical properties with temperature across the boundary layers. If, however, the simplifications used for the integration and asymptotic solutions are applied to the stagnant model, then integration of equation (43) yields

$$q_w = -\int_0^{\delta_t} \phi\theta\lambda\, dy, \tag{45}$$

where δ_t is now the distance from the wall to

the nearest point in the mixture at which the vapor is essentially at the saturation temperature.

The boundary conditions and temperature polynomial profile for the integration and asymptotic solutions may also be applied to the stagnant model by substituting equation (27) into equation (45) to eliminate θ. Integration of the resulting equation yields solutions identical to the asymptotic solutions, i.e. equations (40) and (41). This shows that, if the same approximations are introduced in both cases, the asymptotic and stagnant-model solutions are identical. One can, therefore, conclude (1) that in the fully developed thermal boundary layer, conduction and convection perpendicular to the wall are the major modes of heat transfer, and (2) that convection heat transfer due to motion parallel to the wall is insignificant. Furthermore, inspection of equation (45) reveals that all of the heat transferred from the wall to the fluid is absorbed by the change in phase.

In the preceding analysis, the fluid properties were assumed uniform across the boundary layer. Equations (42)–(44), however, can be solved numerically with fluid properties evaluated at the local vapor temperature at each step of the integration. The boundary conditions for the numerical calculations are then

$$v(0) = 0, \qquad \psi(0) = -q_w, \qquad \theta(\delta_t) = 0,$$
$$\left.\frac{d\psi}{dy}\right|_0 = -\phi\Gamma(\lambda + c_{pv}\Gamma).$$

Figure 4 shows a typical comparison of the temperature profiles across the boundary layer for the stagnant (with variable properties) and the asymptotic solutions. In this case the thermal boundary layer was fully developed, and the integration and asymptotic solutions were almost identical. Fluid properties for the asymptotic solution were evaluated at the arithmetic mean of the wall and saturation temperatures. Maximum difference in the vapor temperatures predicted by the two methods is about 15 per cent of the wall-minus-saturation temperature difference; the wall heat-transfer coefficient according to the stagnant solution is about 15 per cent less than that predicted by the asymptotic solution.

Results of experimental work performed at

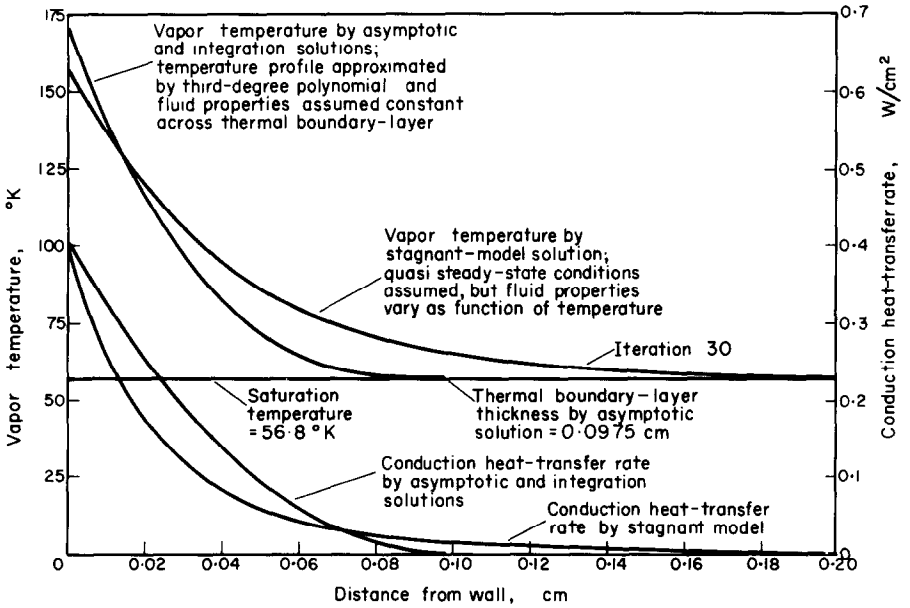

FIG. 4. Typical boundary-layer profiles for nitrogen for a particle Nusselt number of 2·4, shape factor of 1·6, and dia. ~18 μm.

the National Bureau of Standards, Boulder, Colorado, have been compared with the integration, asymptotic, and stagnant-model solutions [6]. Comparisons of experimental wall heat-transfer coefficients with those calculated by means of the asymptotic solution are shown in Figs. 5 and 6 for nitrogen and hydrogen, respectively. Each individual point on Figs. 5 and 6 represents an experimental run. The ranges of key experimental variables are given in Table 2.

The solutions presented in this study, while giving good order of magnitude agreement with experimental results, are not able to account for a trend with wall temperature. The most likely explanation of this is that with increasing wall temperature the particle surface area per unit volume adjacent to the wall is reduced below that which pertains in the free stream. A complete discussion of this and full account of experimental results will be contained in another paper [10].

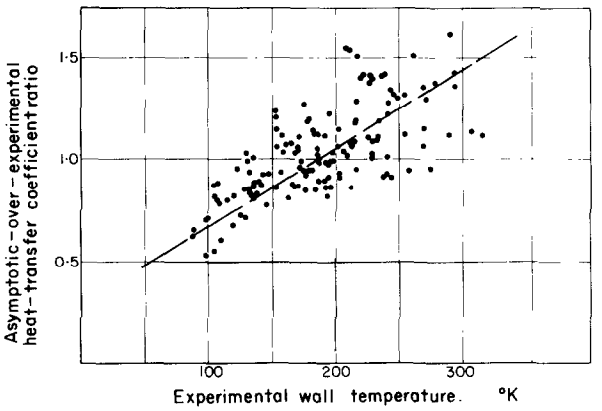

FIG. 5. Heat-transfer ratio vs. wall temperature at 56 cm from orifice for nitrogen for a particle Nusselt number of 2·4, shape factor of 1·6, and diameter ~18 μm. Each individual point represents an experimental run with nitrogen. The ranges of key variables for the runs are given in Table 2.

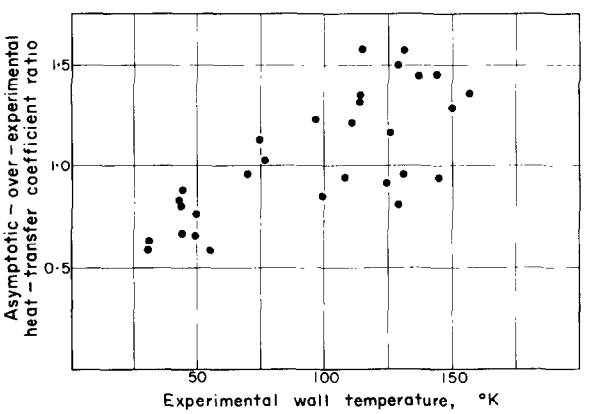

FIG. 6. Heat-transfer ratio vs. wall temperature at 41 cm from orifice for hydrogen for a particle Nusselt number of 2·4, shape factor of 1·7, and diameter ~37 μm. Each individual point represents an experimental run with hydrogen. The ranges of key variables for the runs are given in Table 2.

Table 2. Range of experimental variables

Variable	Nitrogen		Hydrogen	
	Min.	Max.	Min.	Max.
Mixture flow rate, g/s	2·66	4·65	0·79	1·17
Pressure in tube, mm Hg	7·5	46·3	9·0	25·2
Wall heat flux, W/cm^2	0·105	0·672	0·115	1·267

For a rigorous demonstration of the validity of the solutions for a specific system, it is necessary to justify each of the simplifications listed in Table 1 by order-of-magnitude analyses. A less rigorous but simpler method is to calculate the wall heat-transfer coefficient for the vapor alone and compare it with the asymptotic solution. If the asymptotic solution yields a wall heat-transfer coefficient significantly greater (e.g. a factor of two or more) than that for the vapor alone, then change-of-phase dominates the heat-transfer process, and the solutions presented here would most likely provide reasonable results.

In general, the solutions, discussion and conclusions apply to laminar boundary layers. If, however free-stream turbulence is significant, particles from the free stream tend to diffuse into the boundary layer. It is believed for such turbulent boundary layers the solutions presented above may still be applicable, but will tend to underpredict the wall heat transfer coefficient.

CONCLUSIONS

The analyses and forms of the solutions discussed in this paper are summarized in the following conclusions:

1. The thermal boundary layer rapidly reaches an almost constant value and the wall heat-transfer coefficient is considerably greater for a mixture of subliming particles and vapor than for the vapor alone.
2. When the thermal boundary layer becomes fully developed, essentially all of the heat transferred from the wall to the mixture of subliming particles and vapor is absorbed by the change in phase. The reason for this simple energy balance is that, although heat transfer also raises the temperature of the generated vapor from the saturation temperature to the local vapor temperature, convection heat transfer away from the wall by the generated vapor exactly balances the heat absorbed by the generated vapor; thus, the two terms cancel and do not appear in the solutions.
3. The dominant modes of heat transfer in the fully developed thermal boundary layer are conduction and convection away from the wall; convection heat transfer due to motion parallel to the wall is not significant.
4. The wall heat-transfer coefficient in the fully developed thermal boundary layer is directly proportional to the surface area of the particles and, therefore, inversely proportional to particle size for a given particle bulk density.
5. In the fully developed thermal boundary layer the local heat-transfer characteristics depend on the local fluid properties and do not involve the history of the process up to that point. Thus, even though fluid properties in planes parallel to the wall were assumed to be uniform in the development of the solutions, some variation of properties should not affect the results significantly.

ACKNOWLEDGEMENTS

The authors gratefully acknowledge the technical and computing support provided by the Cryogenics Division of the National Bureau of Standards Institute for Materials Research, and the assistance and cooperation of Patricia J. Giarratano in this study. Financial assistance has been provided through the NBS Research Associate Program, The Garrett Corporation, the National Aeronautics and Space Administration, and BUILD, a cooperative program between the University of Colorado and the University of Illinois, sponsored by the Commission on Engineering Education and funded by the C. F. Kettering Foundation.

REFERENCES

1. D. B. CHELTON, B. W. BIRMINGHAM and J. W. DEAN, Solid formation in flowing cryogenic fluids, *Advances in Cryogenic Engineering* (Edited by K. D. TIMMERHAUS), Vol. 8, pp. 311–314. Plenum Press, New York (1963).
2. M. C. JONES, T. T. NAGAMOTO and J. A. BRENNAN, Heat transfer to a subliming solid-vapor mixture of hydrogen below its triple point. *A.I.Ch.E. Jl* **12**, 790–795 (1966).
3. L. FARBAR and C. A. DEPEW, Heat transfer effects to gas-solid mixtures using solid spherical particles of uniform size, *I/EC Fundamentals* **2**, 130–135 (1963).
4. C. L. TIEN and V. QUAN, Local heat transfer characteristics of air–glass and air–lead mixtures in turbulent pipe flow. *Am. Soc. Mech. Engrs* Paper No. 62-HT-65, pp. 1–9, August (1962).
5. R. B. EDELMAN, The flow of a dilute suspension of solids in a laminar gas boundary layer, Ph.D. Dissertation, Yale University, June (1962).
6. A. U. SIMPSON, Forced-convection heat transfer to a mixture of subliming particles and vapor, Ph.D. Thesis, Department of Chemical Engineering, University of Colorado (1967).
7. H. SCHLICHTING, *Boundary Layer Theory*, 4th Edn, McGraw-Hill, New York (1960).
8. R. B. BIRD, W. E. STEWART and E. N. LIGHTFOOT, *Transport Phenomena*, John Wiley, New York (1964).
9. E. R. G. ECKERT and R. M. DRAKE, Jr., *Heat and Mass Transfer*, 2nd Edn, McGraw-Hill, New York (1959).
10. M. C. JONES, PATRICIA J. GIARRATANO and A. U. SIMPSON, Heat transfer to solid-vapor mixtures of cryogens below their triple points flowing through heated tubes, *A.I.Ch.E. Jl*, to be published.

Résumé—On analyse le processus de transport de chaleur vers un mélange à deux phases de particules bien dispersées et en train de se sublimer et de vapeur s'écoulant sur une surface chauffée. On montre par une analyse du type couche limite que, lorsque la surface par unité de volume de la phase particulaire (ou solide) est assez grande, le changement de phase domine le processus de transport de chaleur et hâte le développement de la couche limite thermique. Sous ces conditions, non seulement l'épaisseur de la couche limite thermique devient uniforme à une courte distance en aval du point de départ mais également est considérablement moindre qu'elle devrait être si la phase particulaire était absente. Pour de tels systèmes, les équations décrivant le processus de transport de chaleur peuvent être considérablement simplifiées et, si les propriétés physiques des deux phases sont uniformes, il en résulte une solution remarquablement simple. Pour des systèmes dans lesquels les propriétés physiques ne sont pas uniformes, on expose une solution impliquant une intégration à travers la couche limite. Les solutions sont applicables à des couches limites laminaires sur une plaque plane, en train de s'établir aussi bien qu'à celles entièrement établies; les solutions s'approchent aussi des conditions de l'écoulement à travers un tube, pourvu que le rayon du tube soit grand par rapport à l'épaisseur de la couche limite thermique. Les prévisions de cette analyse théorique sont en accord satisfaisant avec les résultats expérimentaux. La même méthode peut être applicable avec une légère modification à l'écoulement turbulent dans la couche limite.

Zusammenfassung—Der Wärmeübergang von einer beheizten Oberfläche an ein Zweiphasengemisch aus gut verteilten sublimierenden Teilchen und Dampf wird analysiert. Es wird mit Hilfe laminarer Grenzschichtanalyse gezeigt, dass bei genügend grosser Oberfläche pro Einheitsvolumen des Teilchens (oder Festkörpers) die Phasenänderung den Wärmeübergangsvorgang bestimmt und die Entwicklung der thermischen Grenzschicht beschleunigt. Unter diesen Umständen wird die Dicke der thermischen Grenzschicht in geringer Entfernung stromabwärts vom Ausgangspunkt nicht nur gleichförmig, sondern sie ist auch wesentlich geringer als bei fehlender Festphase. Für solche Systeme können die Gleichungen für den Wärmeübergang stark vereinfacht werden und bei einheitlichen Stoffwerten der beiden Phasen ergibt sich eine sehr einfache Lösung. Für Systeme in welchen die physikalischen Eigenschaften nicht einheitlich sind, wird eine Lösung mit einer Integration über die Grenzschicht entwickelt. Die Lösungen lassen sich anwenden, sowohl auf sich ausbildende als auch auf voll ausgebildete laminare Grenzschichten an einer ebenen Platte; die Lösungen gelten angenähert auch für Rohrströmungen unter der Voraussetzung, dass der Rohrradius gross gegen die thermische Grenzschichtdicke ist. Die theoretischen Berechnungen stimmen zufriedenstellend mit den experimentellen Ergebnissen überein. Mit geringen Änderungen könnte möglicherweise die Methode auch auf turbulente Strömung in der Grenzschicht angewandt werden.

Аннотация—Проведен анализ процесса теплообмена при обтекании нагретой поверхности двухфазной смесью тонкодисперсных сублимирующих частиц и пара. При анализе ламинарного пограничного слоя показано, что, когда площадь поверхности на единицу объема частиц (или твердой фазы) достаточно велика, фазовые превращения преобладают над процессами теплообмена и ускоряют развитие теплового пограничного слоя. В этих условиях толщина теплового пограничного слоя становится постоянной на небольшом расстоянии по течению от начальной точки, при чем этот слой значительно тоньше, чем в отсутствии дисперсной фазы. Для таких систем уравнения процесса теплообмена можно значительно упростить, а при постоянных свойствах обеих фаз получается совершенно простое решение. Для систем с неоднородными физическими свойствами получено решение, использующее интегрирование по толщине пограничного слоя. Решения применимы к развивающемуся, а также полностью развитому ламинарному пограничному слою на плоской пластине; решения также аппроксимируют картину течения в трубе при условии большого по сравнению с толщиной пограничного слоя радиуса трубы. Этот теоретический результат удовлетворительно согласуется с экспериментальными данными. С небольшими видоизменениями этот метод, вероятно, может быть применен к турбулентному течению в пограничном слое.